Polyacryloyl Hydrazide: An Efficient, Simple, and Cost Effective Precursor to a Range of Functional Materials through Hydrazide Based Click Reactions

Anuj Kumar, Rewati Raman Ujjwal, Apoorva Mittal, Archit Bansal, and Umaprasana Ojha*

Department of Chemistry, Rajiv Gandhi Institute of Petroleum Technology, Raebareli Ratapur Chowk, UP-229316, India

Ⓢ *Supporting Information*

ABSTRACT: Preparation and studies of ion exchangeable epoxy resins, stimuli responsive hydrogels, and polymer−dye conjugates have been accomplished through hydrazide based click reactions using polyacryloyl hydrazide (PAH) as the precursor. A convenient synthesis of PAH with quantitative functionality was achieved by treatment of polymethyl acrylate with hydrazine hydrate in the presence of tetra-*n*-butyl ammonium bromide. PAH was cured with bisphenol A diglycidyl ether (BADGE) at 60 °C to form transparent resins with superior mechanical properties (tensile strength = 2−40 MPa, Young's modulus = 3.3−1043 MPa, and ultimate elongation = 9−75%) compared to the conventional resins prepared using triethylene tetramine. The resins exhibited higher ion exchange capacities (1.2−6.3 mmol/g) compared to the commercial AHA ammonium-type (Tokuyama Co., Japan) membranes. An azo dye with aldehyde functionality was covalently attached to PAH through hydrazone linkage, and the dye labeled PAH exhibited colorimetric sensing ability for base and acids up to micromolar concentration. The swelling of the PAH based hydrogel varied in the range 4−450% depending on the pH and temperature of the medium. The hydrogels gradually released 30% of the original encapsulated dye in a period of 200 h. PAH−hydroxy naphthaldehyde conjugate released 75% of the original loading in ∼11 days at 37 °C and pH 5.0 through cleavage of the —CONHN=C— linkage. The study depicts the versatility of PAH as a precursor and inspires synthesis of a range of new materials based on PAH in the future.

KEYWORDS: *polyacryloyl hydrazide, epoxy resin, ion exchange membrane, pH sensor, drug delivery matrix, hydrogel*
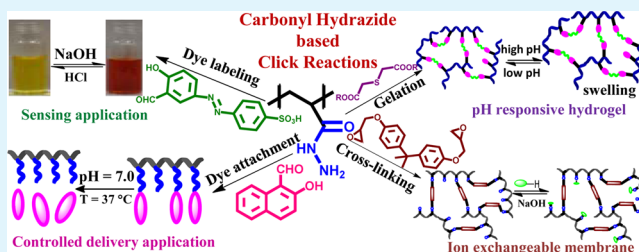
INTRODUCTION

Functional polymers are in the forefront to provide tailored property profiles in many important areas such as drug delivery matrixes,[1,2] sensors,[3,4] sealants, and coating materials.[5] For example, epoxy and amino functionalized polymer based epoxy coatings have shown enhanced fracture toughness and elongation at break compared to the commercial low molecular weight amine and bisphenol A diglycidyl ether (BADGE) based resins.[6,7] Various dye−polymer conjugates have been synthesized to study the chain dynamics,[8] intermolecular association,[9] chemosensing ability,[10] photophysical properties at molecular levels,[11] diffusion kinetics in tissues and living cells,[12] and nanoscale structural transformations. Sumerlin and co-workers have recently reported boronic acid functional block copolymers for sensing of glucose.[13] Hydrophilic polymer supported hydrogels have displayed controlled drug release profiles[14,15] and adequate mechanical properties for applications in biomedical areas[16,17] and enhanced oil recovery. A series of drug delivery matrixes based on acrylate, hydroxy, and amino pendant functionalized polymers have successfully been developed and studied.[18,19] For all the above applications, the ease of synthesis and cost associated with large scale production plays an important role in successful commercial implementation of the above materials.

The reactivity of the carbonyl hydrazide functional group is well documented in the literature.[20,21] This particular functional group reacts rapidly with a range of other functional moieties such as esters, carboxylic acids, aldehydes, acrylates, and epoxides under ambient conditions without use of any additional catalysts. Therefore, carbonyl hydrazide functional polymers offer an exciting option to develop a range of functional materials using click reactions.[22,23] However, considering the promise offered by this class of materials, only a limited number of publications involving functional materials based on polyacryloyl hydrazide (PAH) have been reported so far.[24,25] In the past, carbonyl hydrazide functionalized biodegradable block copolymers have been reported for controlled release of doxorubicin.[26] Bertozzi and co-workers have effectively used PAH for successful synthesis of glycopolymers.[27] However, in the above cases, the hydrazide functionalization was achieved through a multi-step procedure

by preparing reactive intermediates such as acetoxyme and 4-nitrophenyl carboxylate. Therefore, a robust synthesis of PAH using low cost starting materials will significantly motivate the use of this polymer to develop a range of new materials with enhanced commercial value. Polymethyl acrylate (PMA) is commercially available and can be easily synthesized by free radical or controlled polymerization techniques such as reversible addition−fragmentation chain transfer (RAFT), atom transfer radical polymerization (ATRP), and living anionic polymerization.[28,29]

In this article, we report a convenient synthesis of PAH from PMA with quantitative conversion of carboxylates to carbonyl hydrazides. To demonstrate wide applicability of PAH, a range of useful materials including ion exchange epoxy resins, stimuli responsive hydrogels, pH sensors, and polymer−dye conjugates were prepared using various hydrazide based click reactions. The thermo-mechanical properties and ion exchange capacities (IEC) of the epoxy resins were studied. Dye labeling of PAH was investigated using various spectroscopic techniques. Delivery profiles of hydrogels and polymer−dye conjugates were discussed.

■ EXPERIMENTAL SECTION

Materials. Methyl acrylate (s-d fine chem., >99%), *N,N*-dimethyl formamide (DMF, Merck, ≥99.8%), potassium bromate (Merck, >99.0%), sodium hydrogen sulfite (Merck, 58.5−67.4%), sodium chloride (Qualigens, >99.9%), hydrazine hydrate (s-d fine chem., 99%), tetra-*n*-butyl ammonium bromide (TBAB, Merck, ≥98.0%), BADGE (Alfa Aesar, >80.0%), diethyl malonate (DEM, s-d fine chem., 98%), sulfanillic acid (Merck, >99.0%), sodium nitrite (Merck, ≥98.0%), salicyldehyde (SRL chemicals, 99.0%), sodium hydroxide (Qualigens, 98.0%), phenol (Qualigens, 99.0%), potassium hydrogen phthalate (KHP, s-d fine chem., >99%), potassium dihydrogen phosphate (KH_2PO_4, Rankem, ≥99%), hydrochloric acid (HCl, s-d fine chem., 35-38%), potassium chloride (KCl, Himedia, 9.5%), D_2O (Sigma Aldrich, 99.0%), $CDCl_3$ (Sigma Aldrich, 99.8 atom % D), thiodiglycolic acid (Acros Organics, 98.0%), methanol (Qualigens, 99.0%), sulfuric acid (Merck, 98%), ethyl acetate (Merck, ≥99.5%), sodium bicarbonate ($NaHCO_3$, Merck, ≥99.0%), dimethyl sulfonic acid (Merck, 99.5%), triethylenetetramine (TETA, Alfa Aesar, tech. 60%), 2-hydroxy-1-naphthaldehyde (HND, Sigma Aldrich, >99.0%), and rhodamine B (Lobachemie, >95.0%) were used as received. The hexane was purified by refluxing over sulfuric acid for 24 h. They were washed with an aqueous solution of KOH three times followed by distilled water. Then, they were stored over sodium sulfate overnight at room temperature. Finally, the hexane was distilled over CaH_2 under a nitrogen atmosphere before use. Dimethyl 2,2′-thiodiacetate (DTDA) was synthesized from thiodiglycolic acid using a reported procedure.[30] Tetrahydrofuran (THF, Qualigens, 99.0%) was refluxed over sodium metal and benzophenone overnight and distilled under a nitrogen atmosphere prior to use. In a typical purification procedure, the PAH was added to methanol and kept undisturbed until the entire polymer settled down, and the same procedure was repeated with the precipitate three times. Finally, the precipitate was dried in a rotary evaporator under reduced pressure conditions.

Instrumentation. ^{1}H NMR spectroscopy for structural analysis was carried out on a Bruker 500 MHz spectrometer using D_2O or $CDCl_3$ as solvents. ^{1}H NMR spectra of solutions in D_2O or $CDCl_3$ were calibrated to tetramethylsilane (TMS) as an internal standard (δH 0.00). The Perkin Elmer Spectrum Two FT-IR spectrometer was used to record the FT-IR spectra of the samples as either solid or thin film. All the samples were recorded using "attenuated total reflectance" (ATR) mode. The PIKE MIRacle single reflection horizontal ATR accessory equipped with a ZnSe ATR crystal was used for recording the FT-IR spectra. The polymer samples were dissolved in appropriate solvents and kept in a Teflon Petri dish to evaporate the solvent. Solvent cast thin films of the polymers and powdered samples of the

small molecules were pressed against the ATR crystal to record the spectra. The spectra were collected at 4 cm^{-1} spectral resolution utilizing a 1 min data collection time. UV−visible (UV−vis) spectra of the samples were obtained at room temperature on a Lab India UV−vis 3200 instrument. The differential scanning calorimetry (DSC) studies were performed in a METTLER TOLEDO DSC 1 instrument. The samples were recorded at a 10 °C/min heating and cooling rate under a N_2 atmosphere. The glass transition temperatures (T_g) from the first cooling traces of the samples were reported herewith. The thermal gravimetric analysis studies were performed using a Perkin Elmer STA6000 simultaneous thermal analyzer. The thermal stabilities of the cured samples were measured under a nitrogen atmosphere at a 10 °C/min heating rate. The thermal degradation temperature was taken as the onset temperature at which initial weight loss occurred. The tensile studies were performed according to ASTM D638 using an H25K-S UTM Tinius Olsen extensometer. The samples were recorded as rectangular strips at ∼25 °C using a 25 kN load cell and at a crosshead speed of 10 mm/min. The data represented here is an average of three specimens. Inherent viscosities were measured at ∼25 °C using an Ubbelohde viscometer. The inherent and reduced viscosities were extrapolated to zero concentration to determine the intrinsic viscosities of the polymers.

Synthesis of PMA (I). PMA was synthesized using a procedure reported earlier.[31] Methyl acrylate (17.20 g, 2.0 × 10^2 mmol) in 284 mL of H_2O was placed in a 1 L flask, and 5 mL of potassium bromate solution (0.08 g, 0.48 mmol) followed by 5 mL of sodium hydrogen sulfite solution (0.24 g, 2.3 mmol) was added to it. The flask was swirled to mix the contents thoroughly, and the reaction was allowed to proceed for about 15 min. The reaction mixture was then poured into 300 mL of sodium chloride solution (88.0 g, 1.5 × 10^3 mmol) to coagulate the polymer. It was washed with water to remove salt and unreacted monomer. The obtained PMA was dried at ambient temperature under reduced pressure for further use. Yield: 14.0 g, 81.4%. ^{1}H NMR (500 MHz, $CDCl_3$) δ (ppm): 1.3−2.0 (m, 2H, —CH_2—CH—COO), 2.3 (br, 1H, —CHCOO), 3.7 (s, 3H, —COOCH_3). FT-IR (thin film, cm^{-1}): 1158 (s, C—O), 1436 (m, C—H), 1728 (s, C=O), 2852 (w, C—H), 2954 (m, C—H). GPC (THF): M_n = 64000 g/mol, polydispersity index = M_w/M_n = 1.65.

Synthesis of PAH (II). A solution of PMA (10.0 g, 0.156 mmol) in 300 mL of THF was placed in a 1 L round-bottom flask. To it, hydrazine hydrate (38.8 g, 7.6 × 10^2 mmol) and TBAB (10.0 g, 31.02 mmol) were added. The mixture was stirred at 60 °C for 12 h. The reaction mixture was cooled to room temperature and kept undisturbed until the layers separated out. The aqueous layer was transferred into methanol to precipitate the product polymer. The obtained white product was washed with methanol several times to remove the low molecular weight impurities and dried under reduced pressure at ambient temperature. Yield: 9.5 g, 95%. ^{1}H NMR (500 MHz, D_2O) δ (ppm): 1.3−2.2 (m, 3H, —CH_2—CH—CO—), 3.15 (br, 2H, —CONH—NH_2). FT-IR (thin film, cm^{-1}): 981 (m, C—N), 1447 (m, C—H), 1610 (s, C=O), 2924 (m, C—H), 3261 (m, N—H).

Synthesis of Epoxy Resins (III). A typical procedure for PAHER-12 (PAH:BADGE = 1:2, wt:wt) is described below; The PAH (1.0 g, 1.56 × 10^{-2} mmol) was freshly precipitated in methanol and was instantly dispersed in chloroform (15 mL). The degassed BADGE (2.0 g, 5.87 mmol) was added to a PAH and chloroform mixture. The resulting mixture was degassed at 0 °C for 4 h. The mixture was then poured onto the teflon petri dish and cured at 25 °C followed by 60 °C for 24 h each. A similar procedure was followed for other compositions, i.e., PAHER-14, PAHER-16, and PAHER-18.

Viscosity Measurement. The viscosity of PMA was measured in THF and DMF solution. The 1:1 (v:v) ratio of THF and DMF was used as a solvent to prepare a 1−10 wt % polymer solution. The solutions were used to measure the inherent viscosities at ∼25 °C using an Ubbelohde viscometer. The inherent and reduced viscosities were plotted against concentration and extrapolated to zero dilution to determine the intrinsic viscosity (Supporting Information, Figure S1). The same procedure was followed to measure the viscosity of PAH. However, instead of a THF and DMF (1:1, v:v) mixture, a 1.0 wt %

Scheme 1. Synthesis of PAH from PMA and a General Synthetic Strategy to Various Functional Materials Based on PAH
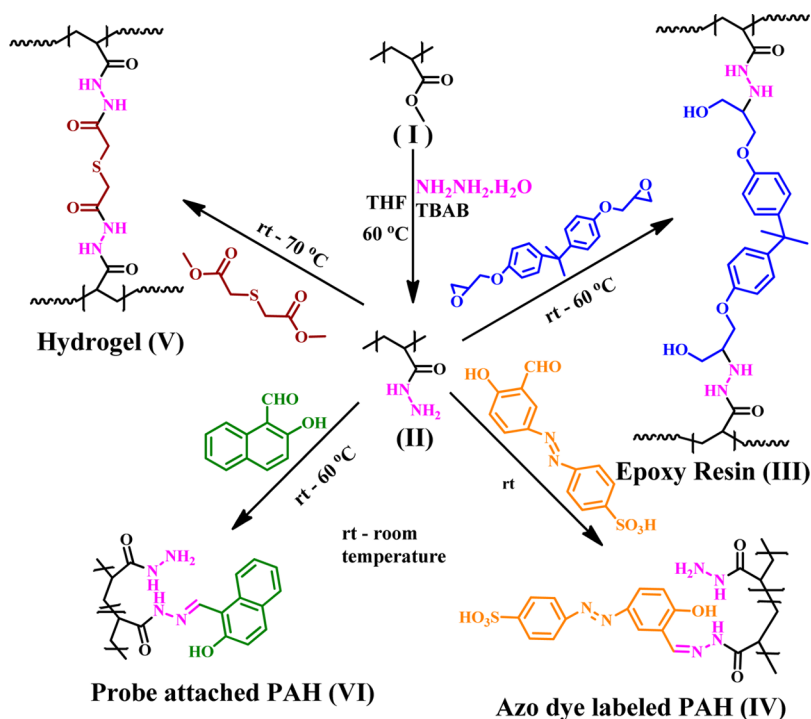
aqueous solution of NaCl was used as the solvent to prepare a 1 to 0.2 wt % PAH solution. NaCl was added to the aqueous solution of PAH to eliminate the possibility of segregation due to intermolecular hydrogen bonding between polymer chains during the measurement.

Procedure for Anion Exchange Study. A certain weighed amount of epoxy resin was dipped in 5×10^3 mmol/L acid (HCl, H_2SO_4, or CH_3COOH) solution at ~25 °C and kept undisturbed for 24 h. The films were then removed and washed repeatedly with water. The anion modified films were immersed in deionized water and titrated against 100 mmol/L NaOH solution using phenolphthalein as the indicator. The end point was determined after three concurrent readings.

The IEC in the case of HCl and CH_3COOH was calculated as follows:

$$\text{NaOH (mmol)} \times \left(\frac{1}{\text{wt}_{\text{resin}} \text{ (g)}} \right) \text{(mmol/g)} \quad (1)$$

where the amount of NaOH (mmol) was determined from titration and wt_{resin} (g) represents the initial weight before dipping the samples in acid solution. In the case of H_2SO_4, eq 1 was divided by 2 to obtain the IEC.

Synthesis of Azo Dyes. The azo dyes were synthesized using a similar procedure reported elsewhere.[32]

4-((3-Formyl-4-hydroxyphenyl)diazenyl)benzenesulfonic Acid (FHBS, $C_{13}H_{10}N_2O_5S$). In test tube A, a solution of water (1.5 mL) and conc. HCl (36%, 1.5 mL) was cooled to 0 °C in an ice bath. In a 50 mL round-bottomed flask, sulfanilic acid (0.87 g, 5.0 mmol), sodium nitrite (0.38 g, 5.50 mmol), and water (1.5 mL) were placed and stirred rapidly. To the stirring mixture, the solution of test tube A was added and stirring was further continued for 10 min. The precipitate formed was filtered and added to a solution of salicyldehyde (0.62 g, 5.1 mmol) and aqueous NaOH (10 mL, 2.5 $\times 10^3$ mmol/L) maintained at 0 °C. After 10 min, conc. HCl (36%, 1.5 mL) was slowly added to the above solution followed by NaCl (1.0 g, 17.1 mmol). The resulting solution was heated for 15 min with continuous stirring. The reaction was cooled to 0 °C, and the solid precipitate was filtered and dried. The obtained product was purified by recrystallization from methanol. This dye was obtained as a yellow solid. Yield: 2.84 g, 92%. mp: 320 °C dec. ^{1}H NMR (500 MHz, D_2O)

δ (ppm): 6.7 (d, 1H, Ar H), 7.6 (d, 2H, Ar H), 7.8 (m, 3H, Ar H), 8.0 (s, 1H, Ar H), 10.0 (s, 1H, —CHO). FT-IR (solid, cm^{-1}): 836 (m, C—H), 1185 (s, S=O), 1471 (m, N=N), 1530 (w, C=C), 1575 (m, C=C), 1690 (m, C=O), 3489 (m, O—H).

4-((4-Hydroxyphenyl)diazenyl)benzenesulfonic Acid (HBS, $C_{12}H_{10}N_2O_4S$). The same procedure as above was followed, only instead of salicyldehyde, phenol was used. This dye was obtained as an orange colored solid. Yield: 2.61 g, 93%. mp: 255 °C dec. ^{1}H NMR (500 MHz, D_2O) δ (ppm): 7.1 (d, 2H, Ar H), 7.9 (m, 4H, Ar H), 8.0 (d, 2H, Ar H). FT-IR (solid, cm^{-1}): 845 (s, C—H), 1171 (s, S=O), 1504 (m, N=N), 1591 (m, C=C), 3458 (m, O—H).

Synthesis of Polymer Dye Conjugate (PAH−FHBS) (IV). The stock solutions of FHBS (4.89 mmol/L) and PAH (0.19 mmol/L) were prepared in water. FHBS solution (0.02 mL, 4.89 mmol/L) and PAH solution (0.5 mL, 0.19 mmol/L) were mixed at room temperature, and the reaction mixture was stirred overnight. The reaction mixture was transferred into methanol to precipitate the product. The precipitate formed was filtered and washed repeatedly with methanol. The yellow solid obtained was dried under reduced pressure. ^{1}H NMR (500 MHz, D_2O) δ (ppm): 1.3−2.2 (m, 3H, —CH_2—CH—CO—), 3.15 (br, 2H, —CONH—NH_2), 6.7 (s, 1H, Ar H), 7.6 (s, 1H, —CH=N—), 7.7 (m, 2H, Ar H), 7.8 (m, 3H, Ar H), 8.1 (s, 1H, Ar H). FT-IR (thin film, cm^{-1}): 846 (w, C—H), 1189 (m, S=O), 1449 (m, N=N), 1530 (m, C=N), 1662 (s, C=O), 2930 (m, C—H), 3048 (m, C—H), 3289 (s, O—H).

Synthesis of Hydrogel (V). To a 3.0 mL aqueous solution of PAH (0.90 g, 1.41×10^{-2} mmol), DTDA (0.70 g, 3.90 mmol) was added and the mixture was stirred until a homogeneous solution formed. The solution was then kept at 70 °C for 3 h. The hydrogel formed was cooled to room temperature and used for further studies.

Synthesis of Polymer Probe Conjugate (PAHHN) (VI). The HND (1.50 g, 8.71 mmol) was dissolved in minimum methanol (1 mL). This solution was transferred into a 100 mL round-bottomed flask containing aqueous solution (15 mL) of PAH (1.50 g, 2.34 $\times 10^{-2}$ mmol) at 60 °C. The mixture was refluxed overnight. The final reaction mixture was transferred into methanol to precipitate the product. The obtained product was further washed with methanol several times and dried under a vacuum at ambient temperature. Yield: 1.95 g, 65%. FT-IR (solid, cm^{-1}): 1467 (s, C=N), 1580 (s, C=C),

1857

dx.doi.org/10.1021/am404837f | ACS Appl. Mater. Interfaces 2014, 6, 1855−1865
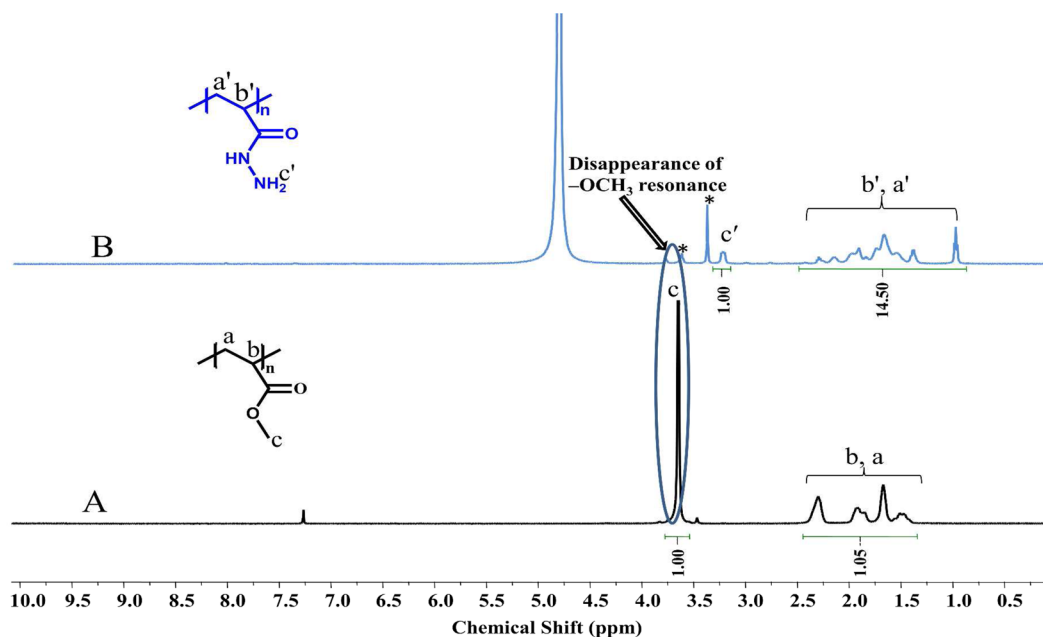
Figure 1. ^{1}H NMR spectra of (A) precursor PMA and (B) PAH. The peaks marked as "*" are due to the presence of adventitious solvent (MeOH) in the polymer.

1604 (m, C=C), 1622 (s, C=O), 2885 (w, C—H), 2977 (m, C—H).

Swelling Ratio Measurement of the Hydrogel. The mass swelling ratio of the gels was determined by a gravimetric procedure. The as synthesized hydrogel was washed with water and weighed prior to the swelling studies. The gel was transferred into a beaker and to it were added different pH solutions. The buffer compositions were as follows: pH 2 (50 mL of 200 mmol/L KCl + 13 mL of 200 mmol/L HCl), pH 4 (100 mL of 100 mmol/L KHP + 0.2 mL of 100 mmol/L HCl), pH 6 (100 mL of 100 mmol/L KH$_2$PO$_4$ + 11.2 mL of 100 mmol/L NaOH), pH 8 (100 mL of 100 mmol/L KH$_2$PO$_4$ + 93.4 mL of 100 mmol/L NaOH), and pH 10 (100 mL of 50 mmol/L NaHCO$_3$ + 21.4 mL of 100 mmol/L NaOH). The mixture was then maintained at ~25 °C for 20 h. After ~20 h, no increase in weight was observed. Free water present on the surface of the hydrogel was removed by soaking with filter paper, and the gel was then weighed. The mass swelling ratio (%) was calculated by the following formula:

$$\frac{wt_{swelled\ gel}\ (g) - wt_{initial\ gel}\ (g)}{wt_{initial\ gel}\ (g)} \times 100$$

A similar study was performed to determine the swelling ratios at 37 and 65 °C.

Encapsulation and Release Procedure of Dye from Hydrogel. The gel was prepared by adding rhodamine B (1.0 × 10^{-3} g, 2.09 × 10^{-3} mmol) to the solution (3.0 mL) of PAH (0.90 g, 1.41 × 10^{-2} mmol) and DTDA (0.7 g, 3.9 mmol). The mixture was then heated at 70 °C for 3 h to get the hydrogel. The hydrogel was repeatedly washed with water to remove the dye present on the surface of the gel. The purified dye encapsulated gel was incubated in a pH 5.0 solution (10 mL) at 37 °C. After a regular time interval, the UV−vis spectra of the incubating solution were checked to estimate the amount of released gel. Quantification of the release efficiency of the dye was estimated by comparing the absorbance of the incubating solution after a certain time period with the absorbance of the fixed amount of dye (1.0 × 10^{-3} g, 2.0 × 10^{-3} mmol) used for encapsulation in the same volume of pH solution (10 mL).

■ RESULTS AND DISCUSSION

The PAH was synthesized from PMA (M_n = 64000 g/mol, M_w/M_n = 1.65), using hydrazine hydrate as the reagent and TBAB as the catalyst (Scheme 1). Initial attempts to synthesize PAH

by reacting PMA with hydrazine hydrate were unsuccessful, since the substitution of —OCH$_3$ by —NHNH$_2$ occurred above 100 °C followed by subsequent cross-linking of the product to yield an insoluble material. Recently, Hedrick and coworkers have reported the efficiency of tetra-n-butyl ammonium salt as a trans-esterification catalyst for hindered carboxylates.[33] Especially in polymeric systems, these quaternary salts are known to facilitate the rate of nucleophilic substitution.[34] When a phase transfer catalyst in the form of TBAB was added to the system, the reaction occurred at lower temperature (60 °C) and PAH was obtained with quantitative conversion of ester to the carbonyl hydrazide. The solubility data, ^{1}H NMR, and FT-IR spectral analysis confirmed the formation of the product. The ^{1}H NMR spectrum of PAH showed disappearance of resonances at 3.7 ppm for the —COOCH$_3$ and 2.3 ppm for the —CHCOO— and appearance of new resonance at 3.15 ppm for the —CONH—NH$_2$, indicating successful substitution (Figure 1). However, the integration value of the resonance at 3.15 ppm was less than that of the calculated value due to rapid deuterium exchange of —NH protons with the solvent (D$_2$O) as documented in the literature for similar cases.[35] The FT-IR spectrum of PAH thin film showed the disappearance of bands at 1728 cm^{-1} for the —C=O$_{str}$ and 1158 cm^{-1} for the —C—O$_{str}$ of ester and appearance of new bands at 1610 cm^{-1} for —C=O$_{str}$ and 981 cm^{-1} for —C—N$_{str}$ of carbonyl hydrazide, suggesting quantitative conversion (Figure 2).

As expected, the polymer was readily soluble in water under all pH conditions and freshly precipitated polymer even dissolved in CHCl$_3$ at low concentration. To check the effect of functional group modification on the molecular weight of the polymer, the intrinsic viscosity (η_{int}) of the precursor in THF/DMF mixture and resulting PAH in saline aqueous solution was measured at ~25 °C. The η_{int} = 0.4 dL/g of PMA was comparable to that of the PAH (η_{int} = 0.49 dL/g), suggesting the chain length remains unaffected during the modification procedure (Supporting Information, Figure S1). The minor difference in the values of η_{int} could be attributed to the strong
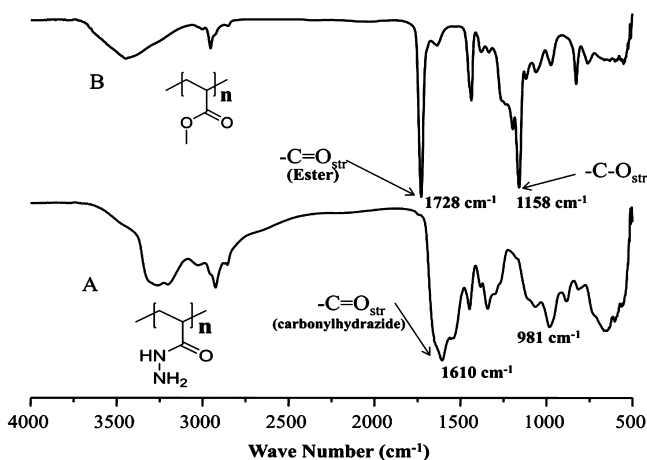
Figure 2. ATR FT-IR spectra of the thin films of (A) PAH and (B) PMA.

hydrogen bond forming ability of PAH in aqueous solution compared to that of the precursor, in which no such behavior is anticipated. Using PAH as the precursor, a set of useful materials were developed and characterized as described in subsequent sections (Scheme 1).

Anion Exchangeable Epoxy Resins (III). Conventional epoxy resins employ low molecular weight amines, such as TETA, as the cross-linker. However, the suitability of these amines is questionable due to their acute toxicity and high cost. Use of PAH as a cross-linker will be advantageous due to the ease of handling and cost effectiveness. A set of epoxy resins were prepared by varying the weight ratio of PAH and BADGE (Scheme 1). The resins were cured at room temperature followed by 60 °C to obtain transparent and defect free films of uniform thickness (Figure 3A).
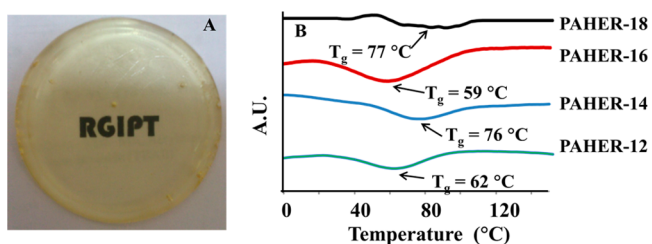

Figure 3. (A) Photograph of PAHER-12. (B) First derivative DSC first cooling traces of epoxy resins recorded at 10 °C/min cooling rate.

The tensile and thermal stability data are tabulated in Table 1. As expected, the ultimate tensile strength (UTS) of the resins decreased and elongation at break increased with an increase in weight ratio of BADGE to PAH and a decrease in the cross-link

density of the networks. The UTS = 40 MPa of the sample with PAH:BADGE = 1:2 (wt:wt) (PAHER-12) was moderately higher than that of the resin (UTS = 31 MPa) prepared using TETA (ER-12). PAHER-18 exhibited excellent elongation at break (75%), though the UTS significantly decreased up to 2 MPa. The Young's moduli of the resins were observed in the range from 1043 to 3.3 MPa, suggesting preparation of coatings with predetermined hardness/softness is possible by varying the PAH:BADGE ratio (Table 1). Interestingly, resin (PAHER-12) prepared using a polymeric amine cross-linker exhibited a significantly higher modulus of 1043 MPa compared to that of the sample (ER-12) prepared using TETA (Young's modulus = 204 MPa). The higher modulus in the case of resins prepared using a polymeric cross-linker could be due to the higher degree of cross-linking and entanglement compared to that of the low molecular weight analogue.[36,37]

The resins exhibited T_g in the range 62−77 °C similar to that of the T_g = 67 °C of precursor PAH, suggesting the thermal processing of these resins may be possible above 80 °C (Figure 3B, Table 1). On heating above 80 °C, the resins became soft and flexible. However, total reshaping of the resins may not be possible due to the presence of inherent cross-links in the sample.

The resins exhibited reversible anion exchange ability due to the presence of free and substituted carbonyl hydrazide moiety (Figure 4). Both the adsorption and desorption of anions occurred under ambient conditions. Two mineral acids (HCl and H_2SO_4) and one organic acid (CH_3COOH) were used for the above purpose. When the thin films of the epoxy resins were dipped in the aqueous solution of the acids, the adsorption occurred gradually over a period of 24 h through formation of $-CONHNH_3^+$ and $-CONHNH_2^{+-}$ ions due to protonation of unsubstituted and N-substituted carbonyl hydrazide moieties present in the resins. The desorption was achieved by simply dipping the acid modified resins in basic pH solutions at room temperature. The extent of loading was estimated by following standard titration techniques.

The resins exhibited average to excellent IEC depending on the mole fraction of BADGE. As expected, the HCl uptake (1.2−6.3 mmol/g) was higher compared to the H_2SO_4 (0.6−1.8 mmol/g) in all the cases due to the bivalency nature of the latter (Figure 5A). PAHER-12 showed higher uptake of HCl and H_2SO_4 compared to PAHER-14 and PAHER-16, whereas in the case of acetic acid no significant difference in all three samples was observed. The experimental IEC = 6.3 ± 0.7 mmol/g of PAHER-12 was comparable to the IECs reported for polyvinyl alcohol and polyallyl amine based resins (4.9 mmol/g) and aminated polypropylene and ethylene diamine based resins (5.1 mmol/g).[38] However, on increasing the BADGE:PAH (wt:wt) ratio, the IEC decreased significantly;

Table 1. Tensile and Thermal Properties of PAH and BADGE Based Epoxy Resins

sample code	PAH (wt %)	BADGE (wt %)	tensile strength (MPa)	elongation at break (%)	Young's modulus (MPa)	onset of decomposition[a] (°C)	T_g[b] (°C)
PAHER-12	33.3	66.6	40	9	1042.8	123	62
PAHER-14	20.0	80.0	26	10	854.2	124	76
PAHER-16	14.3	85.7	18	9	102.9	119	59
PAHER-18	11.1	88.9	2	75	3.3		77
ER-12[c]	33.3	66.6	31	9	204.4	113	

[a]The thermal stability of the polymers was determined from thermal gravimetric analysis. [b]The glass transition temperature was determined from DSC. [c]TETA was used in place of PAH.
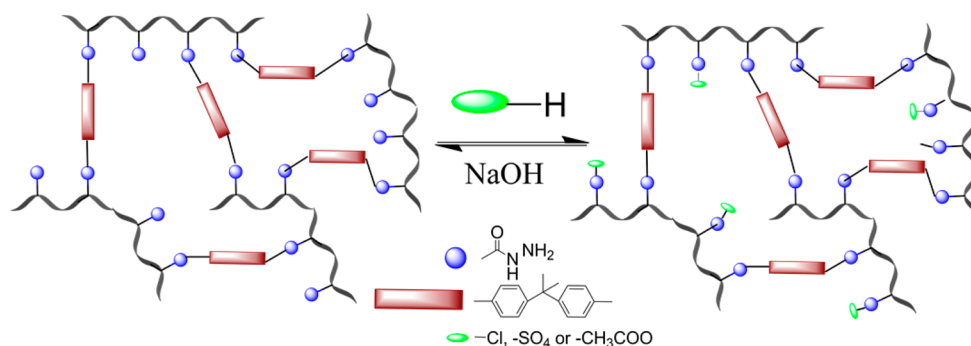
**Figure 4.** Schematics showing the reversible ion exchange process of the epoxy resins.
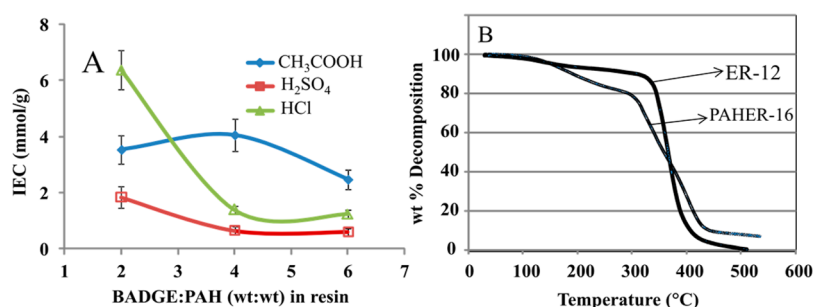
Figure 5. (A) Acid loading capacity of PAHER-12, PAHER-14, and PAHER-16. (B) Thermal gravimetric traces of conventional TETA based resin (ER-12) and PAH based resin (PAHER-16) recorded under a N_2 atmosphere.

i.e., PAHER-14 (IEC = 1.39 ± 0.2 mmol/g) and PAHER-16 (IEC = 1.24 ± 0.2 mmol/g) became comparable to that of the value reported for commercial membranes (AHA ammonium type, Tokuyama Co., Japan, IEC = $1.15-1.25$ mmol/g).[39,40] The higher IEC value of PAHER-12 compared to PAHER-14 and PAHER-16 could be attributed to the presence of unsubstituted $-CONHNH_2$ in the resin, whereas the IEC of PAHER-14 and PAHER-16 was lower due to the presence of sterically hindered mono and di N-substituted carbonyl hydrazides in the resins. The study suggests these resins may be used to removes metal ions, acids, and other acidic impurities from aqueous media along with coating applications.[41]

The thermal stability of the resins was studied under a N_2 atmosphere. The onset of weight loss started above 120 °C, and major weight loss happened above 350 °C (Figure 5B). Similar weight loss behavior was also observed for the conventional resin (ER-12). In the range 120−350 °C, 20% weight loss occurred for the PAH based resins, whereas 10% weight loss was observed for ER-12. In the case of PAHER samples, the additional 10% weight loss above 200 °C compared to that of the ER-12 could be attributed to the cleavage of the carbonyl hydrazide bond as reported before.[42]

Dye Labeling of PAH (IV). Dye labeling of polymers through covalent bond formation is an attractive technique due to the possibility of multiple dye attachment and control over the doping level.[43] However, the efficiency of the process depends on the following factors. The solubility of the polymers in water is preferred to conduct the dye labeling in aqueous media, since most dyes tend to segregate in an organic environment and their photophysical properties get affected.[44] The labeling reaction should be devoid of any post labeling purification and facile enough to provide quantitative conversion.

Herewith, we are reporting a single step instant dye labeling procedure to PAH under mild conditions in the aqueous media. Water-soluble FHBS possessing a $-CHO$ functionality was covalently attached to the PAH using the hydrazone click reaction (Scheme 1). The attachment was monitored and characterized by UV−vis, FT-IR, and ^{1}H NMR spectroscopic techniques. To examine the efficiency of dye labeling, a mixture of FHBS (4.9×10^{-2} mmol/L) and PAH (4.8×10^{-3} mmol/L) was reacted together to ensure that approximately 10 dye molecules are available per polymer chain. However, the above dye concentration will be considered significantly low with respect to the carbonyl hydrazide (FHBS:$-CONHNH_2$ = 1:75, mol:mol) functionality, since one average PAH chain contains approximately 744 $-CONH-NH_2$ groups as per the M_n = 64000 g/mol. The first scan of the PAH−FHBS aqueous solution showed a peak maximum at 380 nm (Figure 6A). This
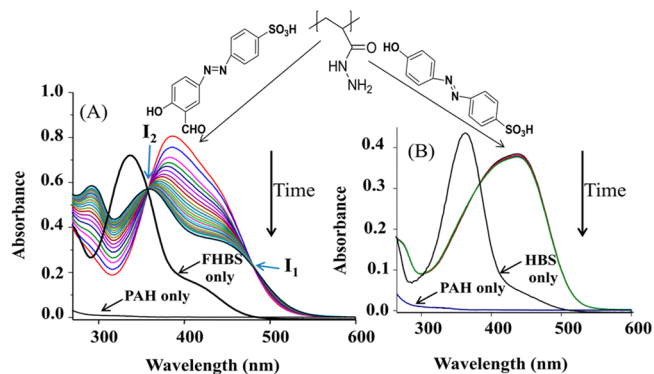
Figure 6. UV−vis traces of the aqueous solution of (A) PAH (4.8×10^{-3} mmol/L) and FHBS (4.9×10^{-2} mmol/L) and (B) PAH (4.8×10^{-3} mmol/L) and HBS (5.3×10^{-2} mmol/L) after different time intervals.
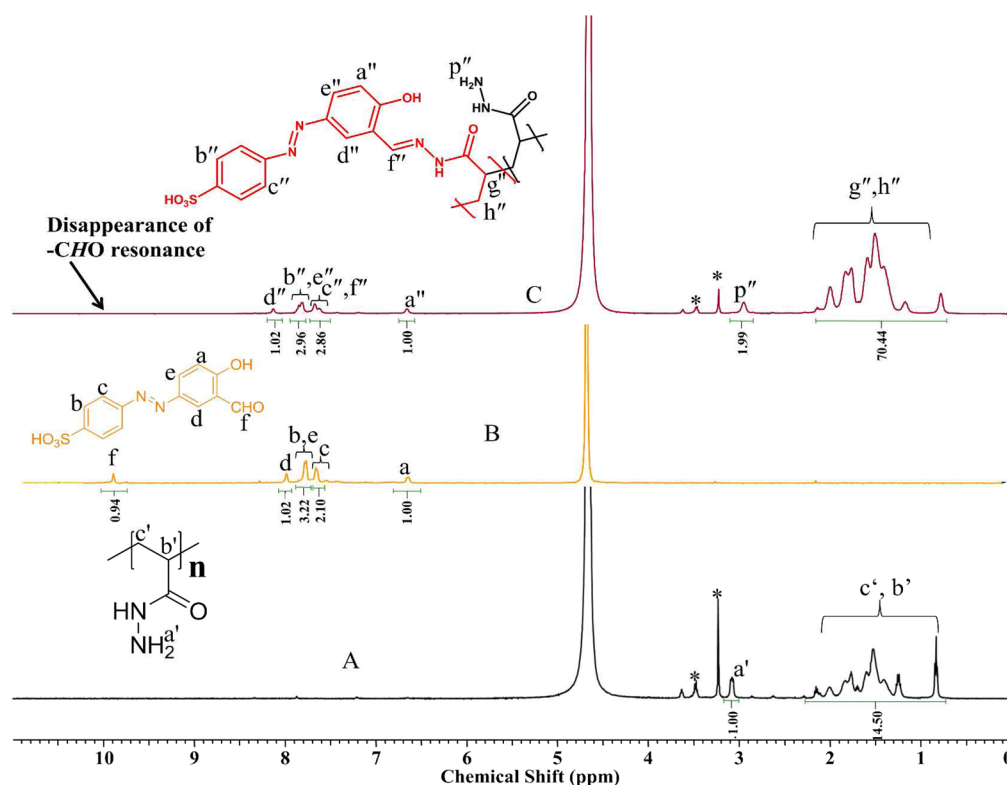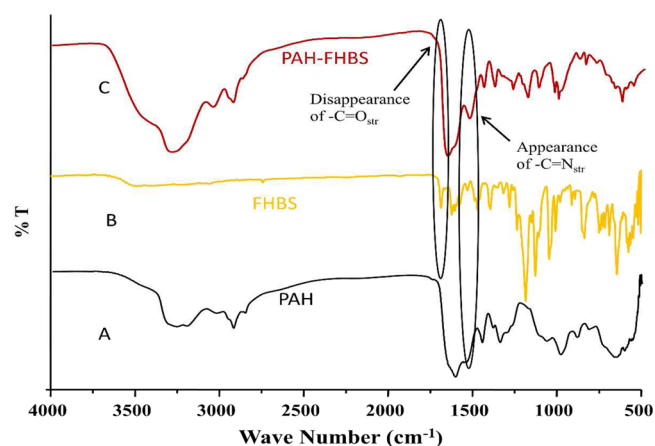
Figure 7. ^1H NMR spectra of (A) PAH, (B) FHBS, and (C) FHBS labeled PAH recorded in D_2O. The peaks marked as "*" are due to the presence of adventitious solvent (MeOH) present in the polymer.

bathochromic shift of λ_{max} by 40 nm compared to the aqueous solution of FHBS could be attributed to the change in pH of the solution due to the presence of PAH. A similar phenomenon was noticed on addition of NaOH to the aqueous solution of FHBS (Supporting Information, Figure S2). With time, the λ_{max} of PAH−FHBS solution gradually shifted to 350 nm and a new peak appeared at 285 nm, indicating covalent attachment of the dye to PAH (Figure 6A). The reaction time was ∼8 min for complete attachment of the dye after which no change in UV−vis trace was noticed. The presence of two isosbestic points further supported the conversion, since two species (*trans*- and *cis*-FHBS) in equilibrium got chemically transformed to a third species (PAH−FHBS) during the process (I_1 and I_2 in Figure 6A). The short reaction time at a low reactant ratio (carbonyl hydrazide:FHBS = 75:1) under ambient conditions indicated the attachment process is highly efficient and any further increase in FHBS concentration will decrease the reaction time. A control experiment was also performed using HBS as the dye devoid of −CHO functionality under similar concentrations. The initial bathochromic shift in the λ_{max} of HBS from 360 to 450 nm was noticed due to the presence of PAH (Figure 6B). However, no noticeable change in the optical behavior with time was observed afterwards, suggesting absence of any chemical transformation. When the dye labeling process was conducted in pH 7.0 buffer solution, the initial shift in λ_{max} of FHBS solution due to addition of PAH was not observed as expected (Supporting Information, Figure S3).

The ^1H NMR spectrum of the aqueous solution of FHBS labeled PAH showed disappearance of resonance at 10 ppm for the −C*H*O and appearance of a new signal at 7.6 ppm for the −C*H*=N−, indicating successful attachment (Figure 7). The ATR FT-IR spectrum of the dye labeled polymer film showed

disappearance of the band at 1690 cm^{-1} for the −C=O$_{str}$ of the aldehyde and appearance of a new band at 1530 cm^{-1} for the −C=N$_{str}$ of the imine linkage, further supporting the UV−vis and NMR spectroscopic data (Figure 8). The doping


Figure 8. ATR FT-IR spectra of powdered (A) PAH, (B) FHBS, and (C) FHBS labeled PAH.

concentration was varied, and the effect of higher PAH concentration on the conformation of azo dye was studied. Interestingly, the cis/trans conformation of FHBS was precisely controlled by varying the concentration of PAH. As can be seen in Figure 9A, the absorbance of λ_{max} at 360 nm accountable to *trans*-FHBS decreased gradually and the absorbance of λ_{max} at 450 nm related to *cis*-FHBS became prominent at a higher concentration of PAH (4.3×10^{-2} mmol/L). Possible reasons for the change in conformation of the azo dye may be explained
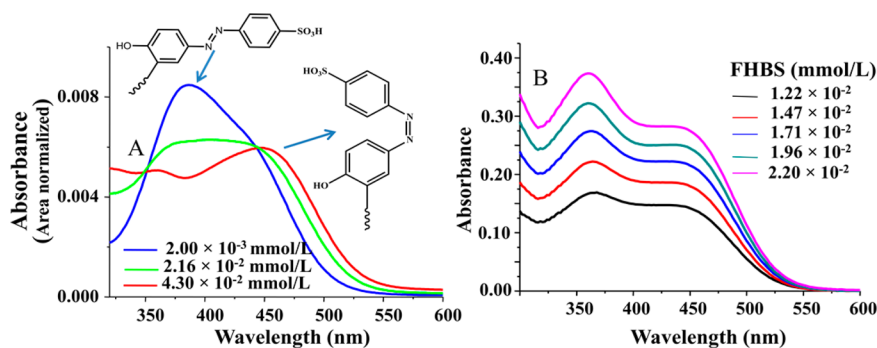
Figure 9. (A) Effect of PAH concentration on the λ_{max} of FHBS (4.2×10^{-2} mmol/L) solution. (B) Effect of FHBS concentration on the λ_{max} of PAH (3.9×10^{-3} mmol/L) solution.
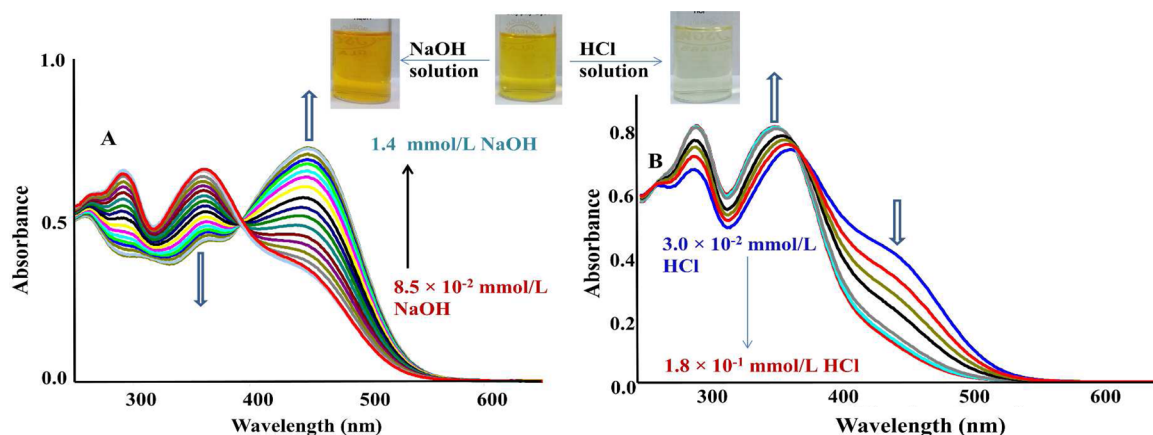
Figure 10. Effect of (A) NaOH and (B) HCl on the λ_{max} of PAH (3.9×10^{-3} mmol/L)−FHBS (4.2×10^{-2} mmol/L) aqueous solution.

as follows. An increase in PAH concentration altered the polarity of the medium and increased the extent of coiling of the polymer chains, forcing the azo dye to adopt an energetically unfavorable cis conformation. A similar phenomenon involving stereoisomerization of azo dye in the polyethylene-solution interface has already been reported before.[45] The effect of FHBS concentration on the optical properties was also investigated keeping the PAH concentration of 3.9×10^{-3} mmol/L constant. As expected, on increasing the FHBS concentration from 1.2×10^{-2} to 2.2×10^{-2} mmol/L, the relative absorbance of the λ_{max} at 360 nm increased from 1.36 to 1.62 with respect to that of the peak at 450 nm, suggesting a gradual increase in the population of the trans conformation (Figure 9B).

Relative absorbance was calculated using the following equation:

$$\frac{^{360}Abs_{[Conc.=X\,mmol/L]} - \,^{360}Abs_{[Conc.=0.012\,mmol/L]}}{^{450}Abs_{[Conc.=X\,mmol/L]} - \,^{450}Abs_{[Conc.=0.012\,mmol/L]}}$$

where $X = (1.47-2.20) \times 10^{-2}$.

This study further revealed that control over conformation is achievable by tailoring the PAH to FHBS ratio in the solution. Due to the presence of −SO₃H and −CONH−NH₂ functionality, the PAH−FHBS conjugate was expected to effectively sense various acids and bases. To ascertain the sensing efficiency in aqueous solution, UV−vis spectra of FHBS labeled PAH were recorded by gradually adding various millimolar solutions of NaOH and HCl. The absorbance of λ_{max} at 450 nm increased gradually, and the absorbance of peaks

at 285 and 360 nm decreased on repeated addition of NaOH (8.5×10^{-2} mmol/L, pH 9.9), with the color of the solution changing from yellow to orange suggesting colorimetric sensing of the base (Figure 10A). The shift in peak maximum and change in color was reversible, as neutralization of pH resulted in reproduction of the original UV−vis trace and retrieval of yellow color. A similar experiment with an organic base, i.e., triethylamine, revealed that the PAH−FHBS conjugate is capable of sensing the organic base at 8.0×10^{-3} mmol/L (Supporting Information, Figure S4). Similarly, on repeated addition of HCl (3.0×10^{-2} mmol/L, pH 4.5) to the PAH−FHBS solution, a small (∼15 nm) hypsochromic shift to λ_{max} at 360 nm and hypochromic shift to λ_{max} at 450 nm was noticed with the disappearance of yellow color, suggesting sensing of the acid (Figure 10B). However, the change was irreversible and increase in pH did not result in any change of optical properties. One possible explanation for irreversibility could be the protonation of the —N=N— group to a stable quinoid structure in a strongly acidic medium (Supporting Information, Scheme S1). Similar mechanisms of protonation resulting in loss of conjugation have been reported earlier.[46,47] On addition of HCl, the intensity of the band at 1449 cm⁻¹ accountable to N=N_str decreased significantly and a new band at 1090 cm⁻¹ for the N—N_str appeared in the FT-IR spectrum (Supporting Information, Figure S5). The absorbance of λ_{max} at 450 nm gradually decreased with an increase in the concentration of HCl in UV−vis spectroscopic analysis (Figure 10B). Disappearance of color and UV−vis and FT-IR spectroscopic data supported the above mechanism. This study signified that PAH−FHBS conjugates may be used to sense acidic pH up to
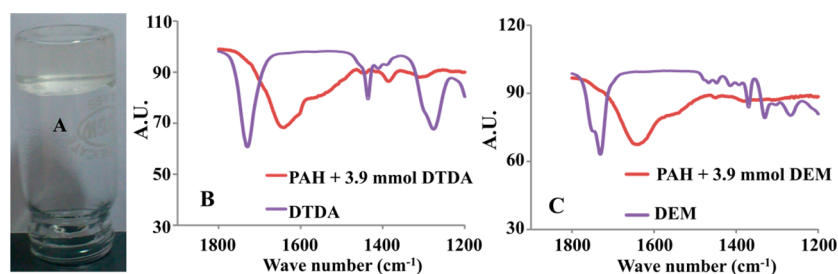
Figure 11. (A) Photograph of a PAH-DTDA hydrogel. (B and C) ATR FT-IR spectra of the cross-linkers and the resulting hydrogels.
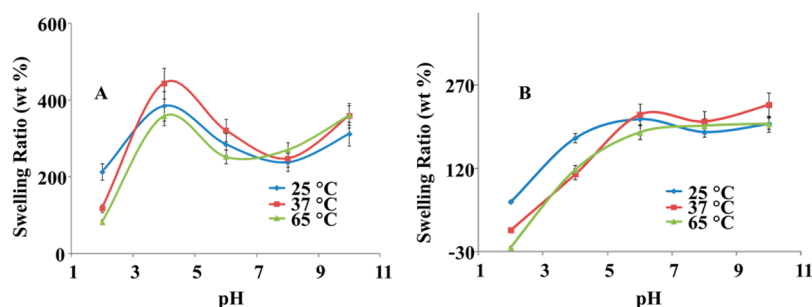

Figure 12. (A) Effect of pH and temperature on the swelling ratio of PAH-DTDA hydrogel. (B) Effect of pH and temperature on the swelling ratio of PAH-DEM hydrogel.

4.5 and basic pH up to 9.9. On further decreasing the basic pH below 9.9 and increasing the acidic pH above 4.5, no noticeable change in the color as well as UV−vis trace was observed. New classes of PAH−dye conjugates may also be prepared by attaching dyes possessing suitable functionality for sensing and related applications.

pH and Heat Responsive Hydrogels for Controlled Delivery (V). In most cases, the cross-linkers used for synthesis of hydrogels are reactive in nature and therefore are associated with stability and handling concerns. In this case, due to swift reactivity of carbonyl hydrazides with stable functional groups such as carboxylic esters, DTDA was used for preparation of hydrogels (Scheme 1).[48] Carboxylic esters are easy to handle, stable to a range of functional groups, and adequately stable under thermal and acidic conditions.[49] The —COOMe of DTDA readily reacted with carbonyl hydrazide at 70 °C to form chemically cross-linked transparent hydrogels (Figure 11A). The FT-IR spectrum of the gel showed disappearance of —C═O$_{str}$ frequency at 1730 cm^{-1} for the ester linkage and appearance of a new band at 1640 cm^{-1} for the —C═O$_{str}$ of the carbonyl hydrazide linkage, suggesting quantitative cross-linking (Figure 11B). The basicity of the —S— linkage present in the structure enhanced the possibility of pH responsiveness of the gels[50] and also rendered the hydrogel a possibility for further structural modifications after formation of gel.[51]

Moreover, —S—(CH$_2$)$_n$—CO— moieties are known for their slow degradation under mild acidic conditions, which could be utilized for various controlled release applications.[52] The swelling was dependent on the temperature and pH of the aqueous solution. In strongly acidic (pH 2) solution, the entire —CONHNH$_2$ moieties got protonated to —CONHNH$_3^+$ ion and therefore the swelling ratio of <200% significantly decreased. On increasing the pH to 4, the swelling ratio increased up to 450% and a similar swelling behavior was measured under strongly basic (pH 10) conditions (Figure 12A). Interestingly, the swelling ratio was 300% for the hydrogel dipped under neutral conditions (pH 7−8). Possibly,

the thioether moiety present in the gel formed a temporary physical cross-linking with the carbonylhydrazide under neutral conditions, increasing the cross-link density through weak van der Waals forces of interaction, which was not possible under strongly acidic or basic conditions. To further verify the hypothesis, a gel was prepared using diethyl malonate (DEM), a diester devoid of —S— unit as the cross-linker. As expected, the swelling behavior was similar for all pH conditions ranging from 5 to 10 (Figure 12B). The overall swelling ratio of PAH−DEM based hydrogel was also lower than that of the gel prepared using DTDA, suggesting thioether moieties are accountable for the swelling ratio and pH responsiveness. At higher temperature (65 °C) and low pH (∼2.0), syneresis was observed in the case of PAH−DEM hydrogel and the swelling ratio value decreased by 30% compared to the initial water content (Figure 12B). The pH and thermal responsiveness indicated the hydrogel can be utilized for controlled delivery applications. To determine the release profile of the hydrogel, rhodamine B was encapsulated in the gel. The dye loaded hydrogel was incubated in aqueous solution at 37 °C and pH 5.0 and the UV−vis spectra of the aqueous solution were recorded after regular time intervals (Figure 13A). The
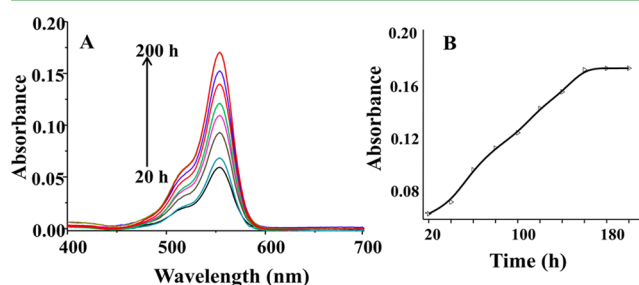
Figure 13. (A) UV−vis spectra of incubating aqueous solution showing a gradual increase in rhodamine B concentration with time. (B) Release profile of rhodamine B from PAH-DTDA hydrogel with time.
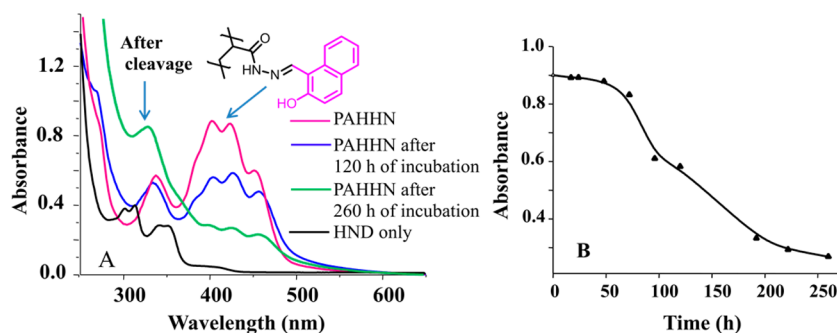
Figure 14. (A) Time dependent UV−vis spectroscopic analysis of the aqueous solution of PAHHN incubated at 37 °C and pH 5.0. (B) Time vs absorbance plot showing the change in the absorbance of the peak at 405 nm with time.

concentration of dye in aqueous media kept on increasing with time, indicating release of dye from the gel due to swelling. The gradual release of the dye continued up to 160 h after which a plateau was reached (Figure 13B).

For quantification, the absorbance of an aqueous solution (0.1 g/L) of rhodamine B was equated with the maximum absorbance reached during the release process and the result indicated 30% release after 200 h. Preparation and studies of PAH based hydrogels using a range of other cross-linkers such as diacrylates, dialdehydes, and acrylic esters are in progress and will be reported soon.

Drug Polymer Conjugate (VI). Drug release by physical encapsulation possesses certain drawbacks in the form of limited loading and release control.[53] An alternative approach is to prepare a polymer−drug conjugate[54,55] and gradually release the drug by cleavage of a chemical bond.[56,57] The second method is more attractive due to their prolonged and uniform release rate. Several reports of drug delivery through cleavage of a hydrazone bond have already been published.[58,59] Therefore, we studied the release capacity of PAH using HND (5.8 mmol/g of PAH) as the probe molecule (Scheme 1). Successful attachment of HND to PAH was confirmed by FT-IR and UV−vis spectroscopic analysis. The band at 1660 cm^{-1} for the —C=O$_{str}$ of the —CHO functionality in HND disappeared, and a new band at 1467 cm^{-1} for the —C=N$_{str}$ of the imine functionality of product indicated successful attachment of HND to PAH (PAHHN) (Supporting Information, Figure S6). The absorption maximum of HND shifted from 325 to 405 nm after treatment with PAH, further suggesting the formation of PAHHN (Figure 14A). The aqueous solution of PAHHN (3.7 × 10^{-7} mmol/L) was incubated at pH 5.0 and 37 °C. The UV−vis spectrum of the solution was recorded at regular time intervals to estimate the extent of degradation. With time, the relative absorbance of the peak at 325 nm increased compared to that of the peak at 405 nm, indicating cleavage of hydrazone linkage and release of the probe (Figure 14A).

The degradation continued up to 260 h after which a plateau for the absorbance of the 405 nm peak with time was noticed, indicating saturation (Figure 14B). From the change in absorbance, 75% release of HND was estimated in 11 days. The delivery kinetics may also be tailored by modifying the hydrophilic and hydrophobic ratio in the above conjugate, and preparation and study of such polymer conjugates based on PAH is in progress.

CONCLUSION

This article demonstrates cost effective large scale production of PAH from PMA with quantitative conversion of functional group. PAH can be utilized to synthesize epoxy resins, hydrogels, dye labeled polymers, and drug delivery matrixes. The epoxy resins can be used for coating as well as acid separation purposes. The dye labeled PAH may be used for sensing as well as controlled delivery applications. The efficiency of the labeling reaction indicates the doping concentration may be controlled precisely targeting a particular application. The hydrogels are promising candidates for delivery as well as enhanced oil recovery applications. The above reported materials may further be modified to optimize the properties. Only a few examples have been stated here as a proof of concept. Development of PAH based block and random copolymers are in progress to fine-tune the properties of developed materials and also production of new materials.

■ ASSOCIATED CONTENT

Ⓢ Supporting Information

The viscosity data of the precursor and PAH, UV−vis spectroscopic data of the PAH in neutral and basic solutions and PAH−FHBS solution in pH 7.0 buffer solution, triethylamine sensing data, ^{1}H NMR spectrum of HBS, and FT-IR spectroscopic data of HCl treated PAH−FHBS conjugate and PAH−HND conjugate. This material is available free of charge via the Internet at http://pubs.acs.org.

■ AUTHOR INFORMATION

Corresponding Author

*E-mail: uojha@rgipt.ac.in. Phone: 0535-270-4221. Fax: 0535-221-1888.

Author Contributions

The article was written through the contribution of all the authors, and all the authors have given approval to the final version of the manuscript.

Notes

The authors declare no competing financial interest.

■ ACKNOWLEDGMENTS

■ REFERENCES

(1) Binauld, S.; Stenzel, M. H. *Chem. Commun.* **2013**, *49*, 2082–2102.

(2) Li, J. *J. Drug Delivery Sci. Technol.* **2010**, *20*, 399–405.

(3) Carlmark, A.; Malmstroem, E.; Malkoch, M. *Chem. Soc. Rev.* **2013**, *42*, 5858–5879.

(4) Roy, D.; Brooks, W. L. A.; Sumerlin, B. S. *Chem. Soc. Rev.* **2013**, *42*, 7214–7243.

(5) Supaphol, P.; Suwantong, O.; Sangsanoh, P.; Srinivasan, S.; Jayakumar, R.; Nair, S. V. *Adv. Polym. Sci.* **2012**, *246*, 213–239.

(6) Tripathy, R.; Ojha, U.; Faust, R. *Macromolecules* **2011**, *44*, 6800–6809.

(7) Arias, M. L.; Frontini, P. M.; Williams, R. J. J. *Polymer* **2003**, *44*, 1537–1546.

(8) Beija, M.; Charreyre, M.-T.; Martinho, J. M. G. *Prog. Polym. Sci.* **2011**, *36*, 568–602.

(9) Breul, A. M.; Hager, M. D.; Schubert, U. S. *Chem. Soc. Rev.* **2013**, *42*, 5366–5407.

(10) Mangold, S. L.; Carpenter, R. T.; Kiessling, L. L. *Org. Lett.* **2008**, *10*, 2997–3000.

(11) Richardson, S. C. W.; Wallom, K.-L.; Ferguson, E. L.; Deacon, S. P. E.; Davies, M. W.; Powell, A. J.; Piper, R. C.; Duncan, R. *J. Controlled Release* **2008**, *127*, 1–11.

(12) Roth, P. J.; Kim, K.-S.; Bae, S. H.; Sohn, B.-H.; Theato, P.; Zentel, R. *Macromol. Rapid Commun.* **2009**, *30*, 1274–1278.

(13) Roy, D.; Sumerlin, B. S. *ACS Macro Lett.* **2012**, *1*, 529–532.

(14) Li, X.; Katsanevakis, E.; Liu, X.; Zhang, N.; Wen, X. *Prog. Polym. Sci.* **2012**, *37*, 1105–1129.

(15) Grover, G. N; Lam, J.; Nguyen, T. H.; Segura, T.; Maynard, H. D. *Biomacromolecules* **2012**, *13*, 3013–3017.

(16) Park, K. M.; Yang, J.-A.; Jung, H.; Yeom, J.; Park, J. S.; Park, K.-H.; Hoffman, A. S.; Hahn, S. K.; Kim, K. *ACS Nano* **2012**, *6*, 2960–2968.

(17) Blanazs, A.; Verber, R.; Mykhaylyk, O. O.; Ryan, A. J.; Heath, J. Z.; Douglas, C. W. I.; Armes, S. P. *J. Am. Chem. Soc.* **2012**, *134*, 9741–9748.

(18) Ossipov, D. A.; Piskounova, S.; Varghese, O. P.; Hilborn, J. *Biomacromolecules* **2010**, *11*, 2247–2254.

(19) Sinkel, C.; Greiner, A.; Agarwal, S. *Macromol. Chem. Phys.* **2010**, *211*, 1857–1867.

(20) Fischer-Durand, N.; Salmain, M.; Rudolf, B.; Juge, L.; Guerineau, V.; Laprevote, O.; Vessieres, A.; Jaouen, G. *Macromolecules* **2007**, *40*, 8568–8575.

(21) Itoh, H.; Suzuta, T.; Hoshino, T.; Takaya, N. *J. Biol. Chem.* **2008**, *283*, 5790–5800.

(22) Schaeffer, G.; Buhler, E.; Candau, S. J.; Lehn, J.-M. *Macromolecules* **2013**, *46*, 5664–5671.

(23) Ganguly, T.; Kasten, B. B.; Bucar, D. K.; MacGillivray, L. R.; Berkman, C. E.; Benny, P. D. *Chem. Commun.* **2011**, *47*, 12846–12848.

(24) Bae, Y.; Nishiyama, N.; Fukushima, S.; Koyama, H.; Yasuhiro, M.; Kataoka, K. *Bioconjugate Chem* **2005**, *16*, 122–130.

(25) Bae, Y.; Fukushima, S.; Harada, A.; Kataoka, K. *Angew. Chem., Int. Ed.* **2003**, *42*, 4640–4643.

(26) Hu, X.; Liu, S.; Huang, Y.; Chen, X.; Jing, X. *Biomacromolecules* **2010**, *11*, 2094–2102.

(27) Kamil, G.; Carolyn, R. B. *J. Am. Chem. Soc.* **2010**, *132*, 9963–9965.

(28) Kwak, Y.; Magenau, A. J. D.; Matyjaszewski, K. *Macromolecules* **2011**, *44*, 811–819.

(29) Toy, A. A.; Vana, P.; Davis, T. P.; Barner-Kowollik, C. *Macromolecules* **2004**, *37*, 744–751.

(30) Agarwal, N.; Hung, C.-H.; Ravikanth, M. *Tetrahedron* **2004**, *60*, 10671–10680.

(31) Badran, A. S.; Abd-El-Hakim, A. A.; Moustafa, A. B.; Abd-El-Ghaffar, M. A. *J. Polym. Sci., Part A: Polym. Chem.* **1988**, *26*, 609–614.

(32) Antony, M. J.; Jayakannan, M. *J. Phys. Chem. B* **2011**, *115*, 6427–6436.

(33) Chan, J. M. W.; Sardon, H.; Engler, A. C.; García, J. M.; Hedrick, J. L. *ACS Macro Lett.* **2013**, *2*, 860–864.

(34) Ojha, U.; Rajkhowa, R.; Agnihotra, S. R.; Faust, R. *Macromolecules* **2008**, *41*, 3832–3841.

(35) Coltelli, M.-B.; Angiuli, M.; Passaglia, E.; Castelvetro, V.; Ciardelli, F. *Macromolecules* **2006**, *39*, 2153–2161.

(36) Wei, K.; Zhu, G.; Tang, Y.; Liu, T.; Xie, J. *J. Mater. Res.* **2013**, *28*, 2903–2910.

(37) Song, L.; Ren, L.; Zhang, M.; Sun, S.; Gao, G.; Gui, Y.; Zhang, L.; Zhang, H. *Ind. Eng. Chem. Res.* **2013**, *52*, 12567–12573.

(38) Nishimura, M.; Higa, M.; Akamine, K.; Masudaya, S. *Desalination* **2008**, *233*, 157–165.

(39) Geraldine, M.; Matthias, W.; Kitty, N. *J. Membr. Sci.* **2011**, *377*, 1–35.

(40) Ye, L.; Zhai, L.; Fang, J.; Liu, J.; Li, C.; Guan, R. *Solid State Ionics* **2013**, *240*, 1–9.

(41) Chakrabarty, T.; Prakash, S.; Shahi, V. K. *J. Membr. Sci.* **2013**, *428*, 86–94.

(42) Shukla, J. S.; Misra, P. K. *J. Macromol. Sci., Part A: Pure Appl. Chem.* **1984**, *21*, 69–76.

(43) Yesodha, S. K.; Pillai, C. K. S.; Tsutsumi, N. *Prog. Polym. Sci.* **2004**, *29*, 45–74.

(44) Zettl, H.; Hafner, W.; Bolker, A.; Schmalz, H.; Lanzendorfer, M.; Muller, A. H. E.; Krausch, G. *Macromolecules* **2004**, *37*, 1917–1920.

(45) Bergbreiter, D. E.; Hein, M. D.; Huang, K. J. *Macromolecules* **1989**, *22*, 4648–4650.

(46) Iwase, A.; Ueda, A.; Kuwae, A.; Hanai, K.; Kunimoto, K. K. *J. Mol. Struct.* **2013**, *1047*, 55–60.

(47) Zainal, Z.; Lee, C. Y.; Hussein, M. Z.; Kassim, A.; Yusof, N. A. *Asian J. Chem.* **2005**, *17*, 1717–1728.

(48) Hou, J.-L.; Shao, X.-B.; Chen, G.-J.; Zhou, Y.-X.; Jiang, X.-K.; Li, Z.-T. *J. Am. Chem. Soc.* **2004**, *126*, 12386–12394.

(49) Yu, J.; Xu, N.; Wei, Q.; Wang, L. *J. Mater. Chem. C* **2013**, *1*, 1160–1167.

(50) Kramer, J. R.; Deming, T. J. *Biomacromolecules* **2012**, *13*, 1719–1723.

(51) Riordan, C. G. *Coord. Chem. Rev.* **2010**, *254*, 1815–1825.

(52) Schoenmakers, R. G.; Van de Wetering, P.; Elbert, D. L.; Hubbell, J. A. *J. Controlled Release* **2004**, *95*, 291–300.

(53) Yu, Y.; Chen, C.-K.; Law, W.-C.; Mok, J.; Zou, J.; Prasad, P. N.; Cheng, C. *Mol. Pharmacol.* **2013**, *10*, 867–874.

(54) Duncan, R. *Nat. Rev. Cancer* **2006**, *6*, 688–701.

(55) Zhu, L.; Zhao, L.; Qu, X.; Yang, Z. *Langmuir* **2012**, *28*, 11988–11996.

(56) Cui, J.; Yan, Y.; Such, G. K.; Liang, K.; Ochs, C. J.; Postma, A.; Caruso, F. *Biomacromolecules* **2012**, *13*, 2225–2228.

(57) Cui, J.; Yan, Y.; Wang, Y.; Caruso, F. *Adv. Funct. Mater.* **2012**, *22*, 4718–4723.

(58) Dong, D.-W.; Xiang, B.; Gao, W.; Yang, Z.-Z.; Li, J.-Q.; Qi, X.-R. *Biomaterials* **2013**, *34*, 4849–4859.

(59) Binauld, S.; Scarano, W.; Stenzel, M. H. *Macromolecules* **2012**, *45*, 6989–6999.

1865

dx.doi.org/10.1021/am404837f | *ACS Appl. Mater. Interfaces* 2014, 6, 1855–1865